Highly porous and stable metal-organic frameworks for uranium extraction

Michaël Carboni,[a†] Carter W. Abney,[a†] Shubin Liu,[b] and Wenbin Lin*[a]

[a]Department of Chemistry, CB#3290, University of North Carolina,

Chapel Hill, NC 27599; wlin@unc.edu

[b]Research Computing Center, University of North Carolina, Chapel

Hill, NC 27599.

Table of Contents

1 - General Experimental:

All solvents were purchased from commercial sources and used without further purification. Thermogravimetric analysis (TGA) was performed in air using a Shimadzu TGA-50 equipped with a platinum pan and heated at a rate of 5 °C per minute under air. ^1H, ^{13}C, and DEPT-135 NMR spectra were recorded on Bruker NMR 400 NB and 400 DRX Spectrometers at 400 MHz. The ^1H spectra were referenced to the proton resonance resulting from incomplete deuteration of deuterated DMSO-d_6 (δ 2.49). The ^{13}C spectra were referenced to deuterated DMSO-d_6 (δ 39.52). Mass spectrometric analyses were conducted using positive-ion electrospray ionization on a Bruker BioTOF Mass Spectrometer. Powder X-ray diffraction (PXRD) patterns were collected on a Bruker SMART APEX II diffractometer using Cu radiation. The PXRD patterns were

processed with the APEX II package using PILOT plug-in. Uranium concentration was determined by UV-Vis measurements using a UV-2401 PC UV-Vis recording spectrometer. Arsenazo(III) dye was used as a chelating agent, binding free U in solution and providing an intense absorption at 652 nm (*Talanta*, **2005**, *66,* 961; *Talanta*, **2010**, *82*, 19). A stock solution of arsenazo III 0.1% (w/v) was prepared to ensure consistency throughout all experiments. Aliquots of supernatant were combined with 40 μL concentrated HNO_3 and 200 μL arsenazo III stock solution prior to thorough mixing and sample analysis. Confirmation of U concentration was obtained with a Varian 820-MS Inductively Coupled Plasma-Mass Spectrometer (ICP-MS). A Hitachi 4700 field emission scanning electron microscope (SEM) was used to determine particle size and morphology. To prepare SEM samples, nanoparticulate dispersions were diluted and thoroughly dispersed in EtOH via sonication. A drop of the dispersion was then placed on glass substrate and allowed to air dry. A Cressington 108 Auto Sputter Coater equipped with a Au/Pd (80/20) target and MTM-10 thickness monitor was then used to coat the sample with a thin conductive layer before taking SEM images. Energy dispersive X-ray spectroscopy (EDS) was used to determine elemental composition of MOF **3**, using an Oxford Instruments 7200 INCA PentaFET×3 Energy Dispersive X-ray Spectrometer. The EDS data were processed with the Inca Microanalysis Suite. Each EDS sample was prepared by placing a powder sample on carbon tape. The spectrometer was referenced to Cu immediately prior to obtaining elemental composition by EDS.
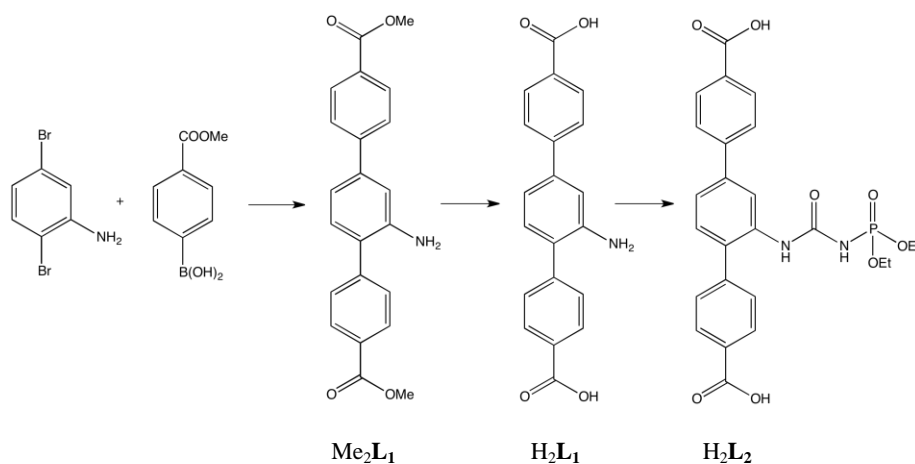
2 – Ligand Synthesis:

Me$_2$**L$_1$**   H$_2$**L$_1$**   H$_2$**L$_2$**

Figure S1: Scheme depicting synthesis of ligands H$_2$**L$_1$** and H$_2$**L$_2$**.

2-1 Synthesis of Me_2L_1: Ligand $Me_2L_1$was prepared by a slighly modified protocol from *Chem. Eur. J.* **2011**, *17*, 6643. Under air- and moisture-sensitive conditions, 2,5-dibromoaniline (0.5 g, 2.0 mmol), 4-(methoxycarbonyl)phenylboronic acid (1.1 g, 6.1 mmol), and CsF (2 g, 1.3 mmol) were dissolved in THF (15 mL). To this solution, 0.15 g (0.7 mmol) of $Pd(OAc)_2$, and 0.4 g (2 mmol) of PPh_3 were added, and the reaction mixture was stirred at 60°C for 48 h. After cooling to room temperature, the reaction mixture was poured into deionized water (25 mL) and the aqueous phase was extracted with CH_2Cl_2. The combined organic phases were concentrated *in vacuo*. The brown solid residue was dissolved in CH_2Cl_2 and purified by silica gel column chromatography. Elution with CH_2Cl_2/Et_2O (50 :1 by volume; Rf = 0.35) gave a slightly yellow solid (0.33 g, 1 mmol Yield : 25 %). ^{1}H NMR (400 MHz, $(CD_3)_2SO$): 8.05 (4H), 7.79 (2H), 7.66 (2H), 7.17 (2H), 7.04 (1H), 5.13 (2H, NH_2), 3.89 (6H, OMe).

2-2 Synthesis of H_2L_1: A suspension of Me_2L_1 (0.33 g, 1 mmol) in THF (65 mL) was heated to 40°C. A solution of KOH in methanol (5.5 $mol.L^{-1}$; 32 mL, 0.18 mol) was added and the reaction mixture was stirred at 40°C for 16 h. The suspension was cooled to room temperature and precipitate was collected by centrifugation. The isolated colorless solid was suspended in THF (25 mL) and 3.3 mL trifluoroacetic acid was added. After the suspension had been stirred for 1.5 h at room temperature, 65 mL of water were added and the yellow solid was isolated, washed with Et_2O and dried *in vacuo* to obtain 0.3 g (0.9 mmol, Yield : 90 %) of slight yellow powder. ^{1}H NMR: (400 MHz, $(CD_3)_2SO$):12.94 (brs, 2H, OH), 8.02 (4H), 7.72 (2H), 7.61 (2H), 7.15 (2H), 7.03 (1H), 5.11 (brs, 2H, NH_2). ^{13}C NMR: (100 MHz, $(CD_3)_2SO$, the signal assignment is in agreement with the DEPT-135 spectrum): 167.63 (COOH) ; 146.20, 144.99, 144.24, 139.96 (C1, C1', C4', C1'') ; 131.31, 130.40, 130.28 (CH); 129.99, 129.56 (C4, C4''); 129.19, 126.96 (CH); 125.07 (C2'); 115.99 (C5'); 114.29 (C3').

2-3 Synthesis of H_2L_2: Under air- and moisture-sensitive conditions, 100 mg (0.3 mmol) of H_2L_1 was dissolved in 5 mL of dry DMSO, to which 1.2 eq. of $OCN-P(O)(OEt)_2$ (0.055 ml, 0.36 mmol) was added. The solution was stirred 24 h at 50°C. The solvent was removed under vaccuum and the product used without further purification. ^{1}H NMR: (400 MHz, $(CD_3)_2SO$): 12.97 (brs, 2H, OH), 8.62 (d, 1H, NH), 8.25 (d, 2H), 8.05 (dd, 4H), 7.81 (d, 2H), 7.52 (d, 2H), 7.38 (d, 1H), 4.45 (1H, NH), 3.98 (q, 6H, CH_2), 1,21 (t, 9H, CH_3). ^{13}C NMR: (100 MHz,

$(CD_3)_2SO$, the signal assignement is in agreement with the DEPT-135 spectrum): 166.97 (COOH); 151.95 (CO); 143.56, 142.14, 139.10, 135.59 (C1, C1', C4', C1''); 132.48 (C4); 129.96, 129.86 (CH) ; 129.82 (C4''), 129.62, 129.20, 126.69 (CH), 122.66, 121.34 (CH5', CH3'), 62.72 (CH_2), 15.76 (CH_3). ESI-MS: m/z $[M+H^+]$= 513.19.

3 - Synthesis of Metal-Organic-Frameworks:

3-1 Synthesis of MOF **1**: 60 mg of $Zr(Cl_4)$ (0.25 mmol), 970 mg of benzoic acid (8 mmol) were dissolved in 12 mL of DMF, aided by 5 minutes of sonication . To this clear solution, 102 mg (0.3 mmol) of H_2L_1 were dissolved and 0.021 mL of water were added. The solution was heated to 70°C for 3 days yielding a white crystaline powder. The solid was collected by centrifugation, followed by washing 5 times with DMF and 3 times with EtOH followed by drying under vacuum.

3-2 Synthesis of MOF **2**: 65 mg of $Zr(Cl_4)$ (0.27 mmol) and 1.05 g (8.6 mmol) of benzoic acid were dissolved in 12 mL of DMF, aided by 5 minutes of sonication. To this clear solution, 100 mg (0.32 mmol) of H_2L_2 were dissolved. The solution was heated to 70°C for 3 days. The solvent was collected by centrifugation and the resulting material was washed 5 times with DMF and 3 times with EtOH prior to drying under vacuum.

3-3 Synthesis of MOF **3**: 60 mg of MOF **2** was suspended in 4 mL of CH_2Cl_2, to which 0.240 mL of Me_3SiBr was added. After 12 hours, the material is isolated by centriguation, washed with CH_2Cl_2 and and dispersed in CH_2Cl_2. 1 mL of water was added and the solution was stirred for an additional 1 hour. The material was isolated by centrifugation, washed 3 times with DMF and 3 times with EtOH before drying under vacuum.

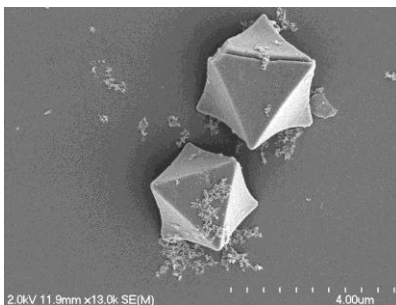## 4 - Characterization of Materials:

4-1 SEM analysis:
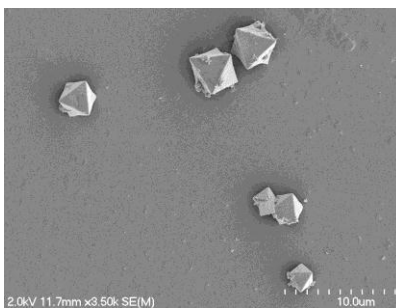
Figure S2: SEM of MOF **1**.

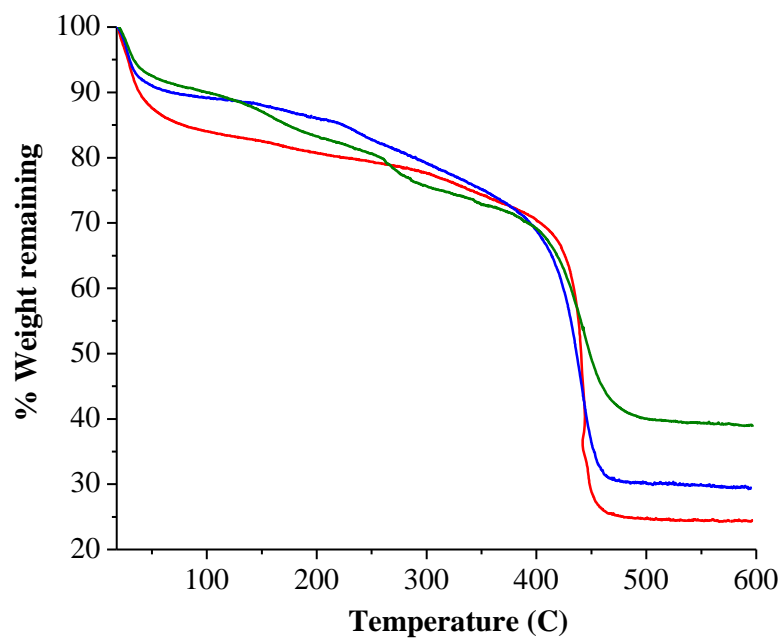**Figure S3:** SEM of MOF **3**.

4-2 TGA analysis:

Figure S4: TGA analysis of MOF **1** (green), MOF **2** (red) and MOF **3** (blue).

Table S1: Comparison between measured and calculated TGA mass loss (%)

%	MOF 1			MOF 2			MOF 3		
	Calculated	Synthesized	Corrected	Calculated	Synthesized	Corrected	Calculated	Synthesized	Corrected
Guest	-	17	-	-	19	-	-	14	-
Linker	68	44	53	77	56	70	74	56	65
Residue	32	39	47	23	24	30	26	30	35

4-3 N_2-uptake and Surface Area Analysis: The analyses were made with about 20 mg of MOF washed successively with DMF, methanol, CH_2Cl_2 and benzene. The MOF was allowed to soak overnight in benzene to ensure complete exchange of solvent. The benzene-filled material is frozen at 0 °C and solvent is sublimed under vacuum overnight. The MOF is further desolvated by heating for an additional 18 hours at 60 °C under vaccuum.
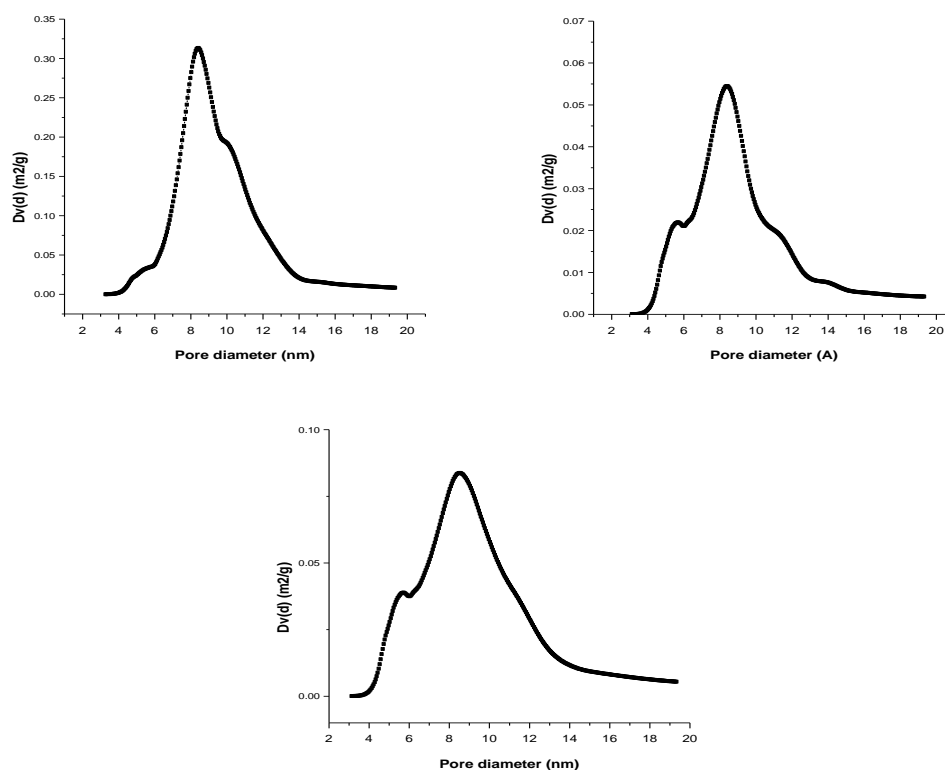

Figure S5: Top: Pore size distribution for MOF **1** (left), MOF **2** (right). Bottom: Pore size distribution for MOF **3**.

4-4 EDS analysis
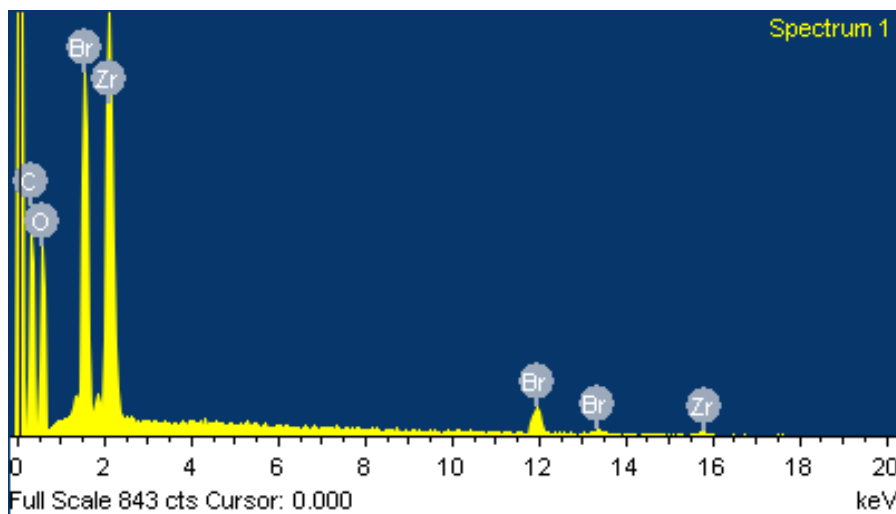
Figure S6: EDS analysis of MOF **3**.

4-5 Dye Uptake Experiment. Fresh crystals of MOFs (10 mg) were isolated by centrifugation after synthesis. After washing the material with DMF and ethanol, the materials were soaked overnight in a 1:1 water:methanol solution of 24 mM dye (Brilliant Blue R-250 or Eosin Y, 24 mM, 2 mL). The resulting colored crystals were washed with water thoroughly until supernatant was colorless. The washed samples were dried under vaccuum and analyzed by TGA.

With Brilliant Blue R 250 (BBR-250):
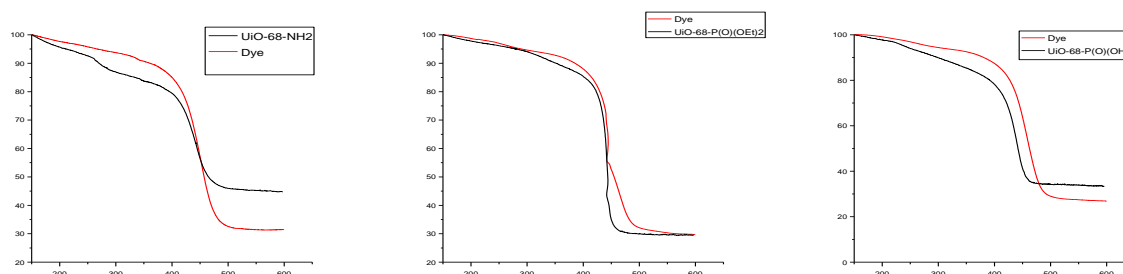
MOF-**1** = 29.6 %, MOF-**2**= 0 %; MOF-**3** = 19.6 %

With Eosin Y:
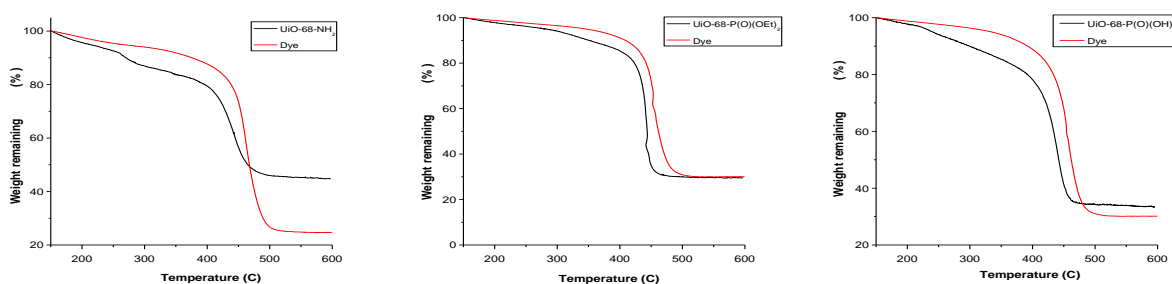
MOF-**1** = 44.84 %, MOF-**2** = 0 % ; MOF-**3** = 9.99 %

Figure S7: TGA analysis of Dye experiments with BBR-250 and Eosin Y.

4-6 Simulation of BET Surface Area and Determination of Solvent Accessible Volume

Simulation of N_2 uptake for MOFs **1-3** was performed with Materials Studio version 5.0.0.0. The sorption calculation module was used, with the task set to Adsorption Isotherm and the method to Metropolis. The unit cells for MOFs **1-3** were packed with N_2 molecules from a starting pressure of 0.0001 kPa to 100 kPa at a temperature of 77 K. Equilibration steps were set to 2500000, production steps were set to 100000, fugacity steps were set to 40, and the sorption isotherm was set to logarithmic. Simulated surface areas were obtained by plotting a linearized BET equation over the partial pressure region of $0.05 < P/P_0 < 0.35$, the slope of which equals the volume of a monolayer of N_2. To improve precision, calculations were performed using the slope and intercept equations of Microsoft Excel 2010, version 14.0.6123.5001. Linear regressions over the described range provided correlation coefficients greater than 0.9990 for all three MOFs. The adsorption cross section used for N_2 at 77K was 0.16 nm^2.

Porosity in MOFs **1-3** was calculated with PLATON v 1.16, build date 05/29/2011 using the SOLV subroutine to determine potential solvent-containing voids.

4-5 MOF Deprotection Study.

MOFs **2** and **3** were thoroughly washed with water before digestion in d_6-DMSO with 0.1 M D_3PO_4 and subsequent analysis by ^1H NMR. Integrated values of the ethoxy protons were compared to integrations in the aromatic region to determine the percent deprotected. Peaks

observed at δ = 7.95 and 7.50 can be assigned to benzoic acid bound to site defects in the Zr SBU.

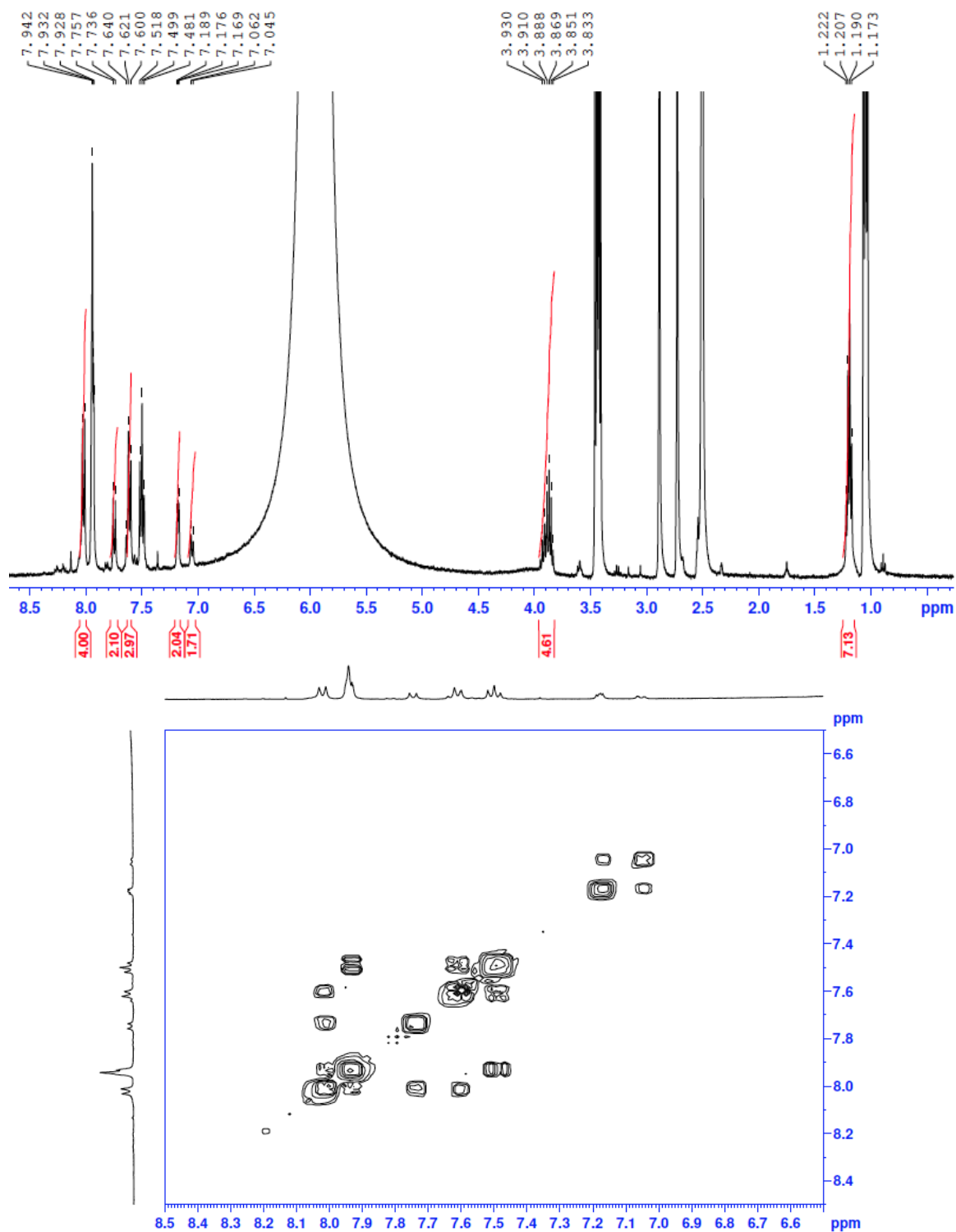**Figure S8:** ^{1}H NMR of digested MOF **2** (top) and ^{1}H COSEY NMR (bottom).
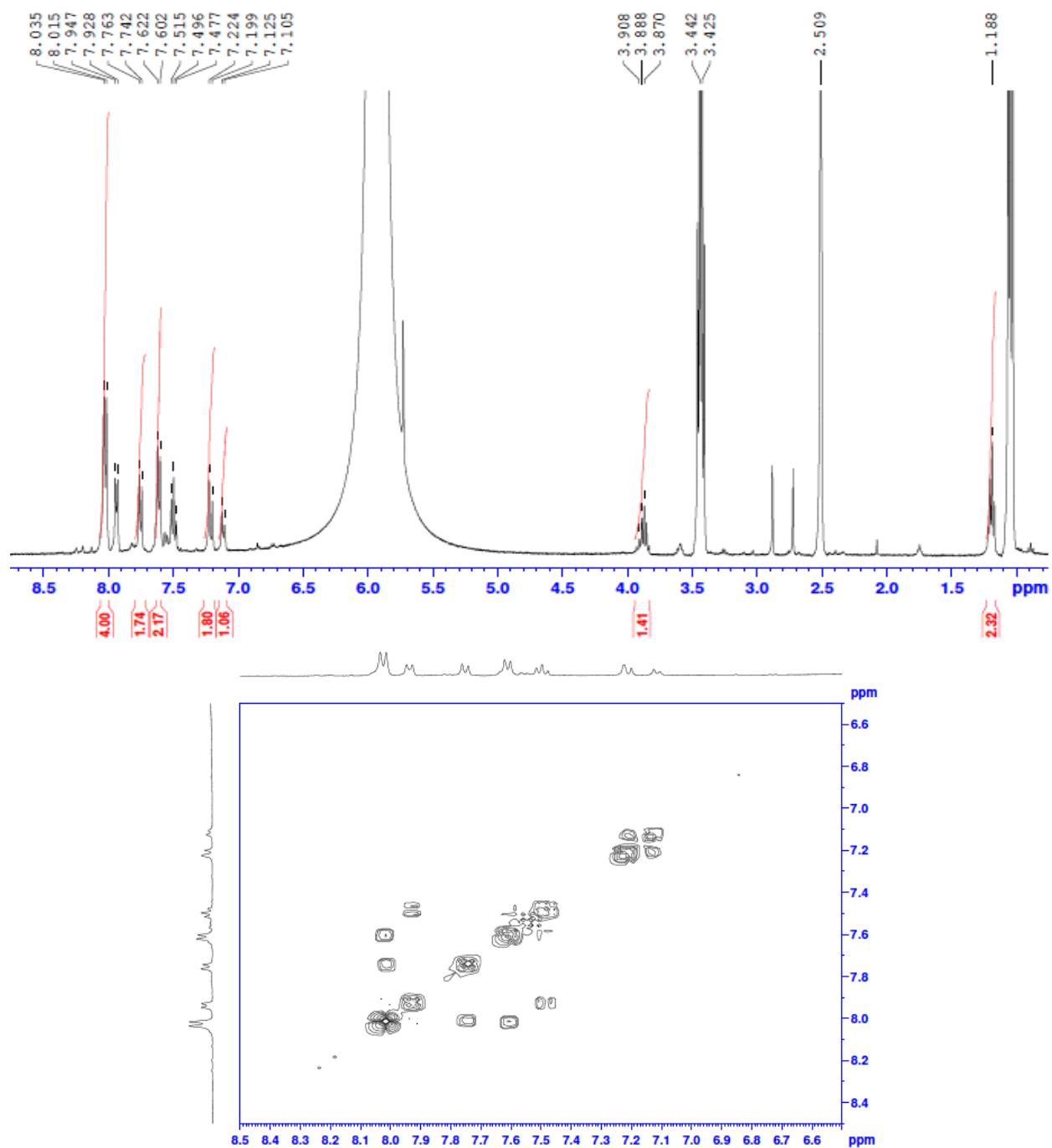
Figure S9: ^{1}H NMR of digested MOF **3** (top) and ^{1}H COSEY NMR (bottom).

5 - Uptake of uranyl in solution of water: [U] = 5 ppm, pH = 2.5, m = 10 mg and V = 10 mL

5 – 1 Methodology

A stock uranium(VI) solution ([U] = 100 ppm) was prepared with uranyl acetate in nanopure water. Solution pH was adjusted to 2.5 (±0.1) using HCl (3 M) solution to avoid precipitation of uranyl at higher pH. In a typical sorption experiment, 10 mg of sorbent was added to 10 mL of U solution at the desired concentration in a high-density polyethylene bottle (previously cleaned with 5 % HNO_3 and rinsed three times with nanopure water). The solutions were shaken at 300 rpm for 1 hour using a PRO Scientific VSOS-4P orbital shaker. The sorbent was separated via centrifugation for 15 minutes at 12000 rpm. An aliquot of supernatant was analysed by UV-vis spectroscopy. A sample of U solution without sorbent material was analyzed during each sorption experiment as a negative control. The sorption capacity (q_e (mg/g)) of U(VI) was calculated with the following equation:

$$q_e = \frac{(C_0 - C_e)V}{m}$$

where C_0 and C_e are the concentration of U(VI) initially and at equilibrium, respectively. V is the volume of solution, and m is the mass of sorbent in solution.

5-2 Desorption studies

The U adsorbed in the UiO materials was eluted by washing with 0.01 M; 0.1 M and 1 M HCl aqueous solutions, successively. The elution step consists of the addition of 10 mL of HCl solution followed by sonication to complete suspension (approximately 10 minutes) and collection by centrifugation (15 minutes at 12000 rpm). This experiment was repeated with 0.1 M and finally with 1 M HCl. U concentration in the washing solution was determined by UV-Vis, as described previously.

5-3 Sorption studies with amidoxime Fibers:
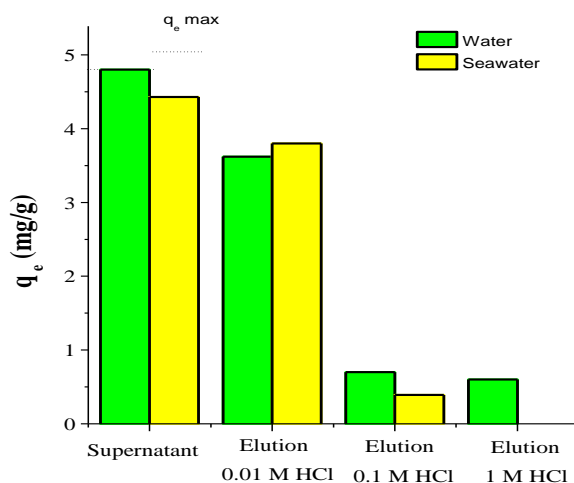
Figure S8: Sorption and desorption studies under the same conditions as the MOFs for amidoxime fibers.

5-3 Isotherms: Langmuir sorption isotherms were obtained by slight modification of the process for sorption experiments. Samples of 10 mL water or artificial seawater were prepared with uranyl concentrations of 30, 60, 80, 100, 150, 200, 250 and 300 ppm at pH 2.5. 10 mg of sorbent was added to each sample and shaken as described previously. Sorbent was separated by centrifugation, and U concentration in the supernatant was determined by UV-vis spectroscopy.

Table S2: Langmuir parameters obtained for MOF-**2** and MOF-**3** in water and artificial seawater at pH=2.5

Langmuir parameters	q_{max} (mg/g sorbent)	K_L (L/mg)	R^2
Water			
MOF **2**	217.4	0.644	0.995
MOF **3**	108.9	0.079	0.964
Seawater			
MOF **2**	188.3	0.092	0.975
MOF**3**	32.5	0.063	0.960

Table S3: Langmuir parameters obtained for MOF-**2** in water at pH = 5

Langmuir parameters	q_{max} (mg/g sorbent)	K_L (L/mg)	R^2
MOF **2**	179.2	0.058	0.961

Figure S9 : Isotherms for MOF **2** and **3** in water at pH 5 (left) and corresponding Langmuir plot for MOF **2** (right).
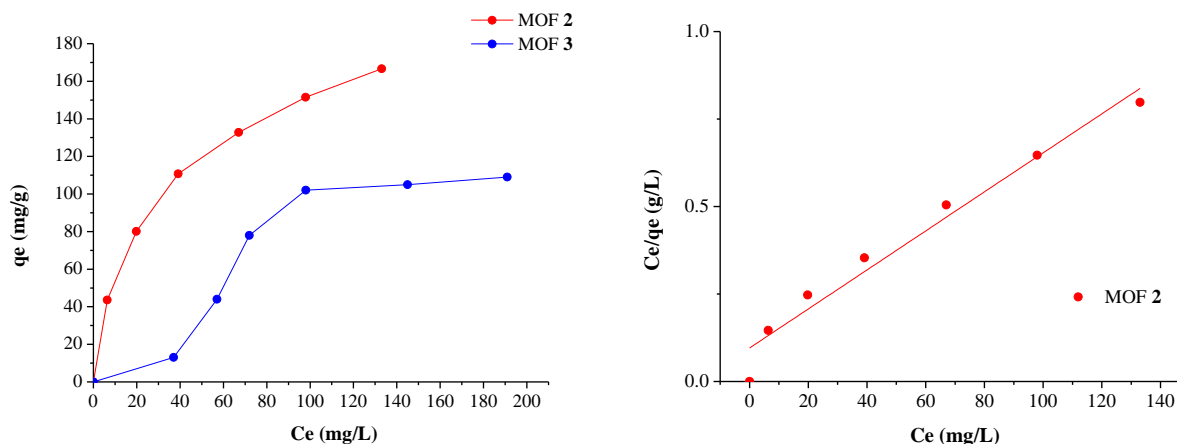
The Langmuir model was used for monolayer sorption on a homogeneous surface with identical sorption sites and no interaction between sorbed particles. MOF **3** at pH 5 does not meet the necessary conditions for modeling with the Langmuir equation, as demonstrated by the Giles type-S classification. The sigmoid curve results from more facile adsorption with increasing concentration, ultimately reaching a plateau at saturation capacity (q_{max}). The observed isotherm likely results from Br in the MOF channels being forced out as U concentration increases, yielding the observed facilitation of binding at higher concentrations as more binding sites are made available. Values for q_{max} for MOF **3** were obtained by averaging the values observed at the plateau.

The Langmuir model is expressed by the following equation:

$$\frac{C_e}{q_e} = \frac{1}{K_L q_{max}} + \frac{C_e}{q_{max}}$$

K_d, the distribution coefficient, was calculated by the following equation:

$$K_d = \frac{C_o - C_e}{C_e} \times \frac{V}{m}$$

K_L is the Langmuir constant

Table S4: Values of the distribution coefficients (K_d in ml/g) for MOF **2** and **3** in water and artificial seawater at pH=2.5

S13

	MOF 2				MOF 3			
	Absorption	0.01 M HCl	0.1 M HCl	1 M HCl	Absorption	0.01 M HCl	0.1 M HCl	1 M HCl
Water	**499000**	**8803**	**650**	**196**	**130560**	**24000**	**1808**	**560**
Seawater	**32300**	**26800**	**880**	**380**	**24000**	**19000**	**1350**	**540**

6 – Computational Data

Table S5: Gas Phase Stability Data for $[UO_2^{2+}(L)_x(OH_2)_y)]^z$ Complexes as Determined by DFT Calculations

Motif	Charge per L	ΔH (kcal mol^{-1})
I	---	-34.62
II	---	-35.83
III	---	-20.99
I-I	---	-58.13
II-II	---	-64.52
III-III	---	-34.94
I-II	---	-59.48
I-III	---	-46.92
II-III	---	-50.13
I*	-1	-188.89
II*	-1	-205.97
III*	-1	-186.96
I-I*	-1	-293.66
II-II*	-1	-312.18
III-III*	-1	-291.37
I-III*	-1	-289.59
II-III*	-1	-307.78

Table S6: Geometrically Optimized Average Bond Lengths (Å) for $[UO_2^{2+}(H_2O)]^{2+}$ in Gas Phase and Solvated

	U=O	**U-OH$_2$**
Calculated	1.748 / 1.758	2.492 / 2.459
EXAFS[1]	1.76	2.41

Literature[2]	1.753	2.484

.../... refers to the results obtained by calculations in the gas phase and solvated with a polarizable conductor calculation model

Table S7: Geometrically Optimized Bond Lengths (Å) for Gas Phase UO_2^{2+} Complexes

Motif	U=O	U-OH$_2$ (Avg)	C(O)$_1$ – U	P(O)$_1$ – U	C(O)$_2$ – U	P(O)$_2$ – U
I	1.755	2.496	2.357	---	---	---
II	1.754	2.495	---	2.373	---	---
III	1.755	2.504	2.384	2.403	---	---
I-I	1.762	2.498	2.391	---	2.386	---
II-II	1.762	2.476	---	2.366	---	2.445
III-III	1.758	2.492	2.437	2.409	2.429	2.441
I-II	1.760	2.499	2.389	---	---	2.401
I-III	1.761	2.474	2.386	---	2.444	2.430
II-III	1.759	2.479	---	2.371	2.467	2.417
I*	1.771	2.482	2.375	---	---	---
II*	1.765	2.516	---	2.239	---	---
III*	1.767	2.561	2.359	2.236	---	---
I-I*	1.775	2.492	2.354	---	2.308	---
II-II*	1.770	2.508	---	2.395	---	2.316
III-III*	1.779	2.560	2.461	2.282	2.398	2.384
I-III*	1.783	2.488	2.344	---	2.500	2.268
II-III*	1.781	2.518	---	2.305	2.453	2.298

Table S8: Geometrically Optimized Bond Lengths (Å) for Solvated UO_2^{2+} Complexes

Motif	U=O	U-OH$_2$ (Avg)	C(O)$_1$ – U	P(O)$_1$ – U	C(O)$_2$ – U	P(O)$_2$ – U
I	1.763	2.473	2.350	---	---	---
II	1.763	2.473	---	2.351	---	---

III	1.764	2.471	2.390	2.374	---	---
I-I	1.767	2.490	2.369	---	2.371	---
II-II	1.772	2.465	---	2.378	---	2.366
III-III	1.768	2.465	2.407	2.405	2.405	2.423
I-II	1.768	2.484	2.368	---	---	2.369
I-III	1.768	2.494	2.373	---	2.386	2.403
II-III	1.768	2.466	---	2.371	2.413	2.403
I*	1.767	2.475	2.317	---	---	---
II*	1.771	2.494	---	2.252	---	---
III*	1.772	2.497	2.381	2.284	---	---
I-I*	1.778	2.483	2.326	---	2.337	---
II-II*	1.778	2.499	---	2.327	---	2.347
III-III*	1.781	2.529	2.423	2.327	2.390	2.359
I-III*	1.782	2.503	2.353	---	2.409	2.309
II-III*	1.786	2.510	---	2.305	2.399	2.322

Complete citation for reference #58: Gaussian 09, Revision A.2, Frisch, M. J.; Trucks, G. W.; Schlegel, H. B.; Scuseria, G. E.; Robb, M. A.; Cheeseman, J. R.; Scalmani, G.; Barone, V.; Mennucci, B.; Petersson, G. A.; Nakatsuji, H.; Caricato, M.; Li, X.; Hratchian, H. P.; Izmaylov, A. F.; Bloino, J.; Zheng, G.; Sonnenberg, J. L.; Hada, M.; Ehara, M.; Toyota, K.; Fukuda, R.; Hasegawa, J.; Ishida, M.; Nakajima, T.; Honda, Y.; Kitao, O.; Nakai, H.; Vreven, T.; Montgomery, Jr., J. A.; Peralta, J. E.; Ogliaro, F.; Bearpark, M.; Heyd, J. J.; Brothers, E.; Kudin, K. N.; Staroverov, V. N.; Kobayashi, R.; Normand, J.; Raghavachari, K.; Rendell, A.; Burant, J. C.; Iyengar, S. S.; Tomasi, J.; Cossi, M.; Rega, N.; Millam, J. M.; Klene, M.; Knox, J. E.; Cross, J. B.; Bakken, V.; Adamo, C.; Jaramillo, J.; Gomperts, R.; Stratmann, R. E.; Yazyev, O.; Austin, A. J.; Cammi, R.; Pomelli, C.; Ochterski, J. W.; Martin, R. L.; Morokuma, K.; Zakrzewski, V. G.; Voth, G. A.; Salvador, P.; Dannenberg, J. J.; Dapprich, S.; Daniels, A. D.; Farkas, Ö.; Foresman, J. B.; Ortiz, J. V.; Cioslowski, J.; Fox, D. J. Gaussian, Inc., Wallingford CT, 2009.

References

1. P. G. Allen, J. J. Bucher, D. K. Shuh, N. M. Edelstein and T. Reich, *Inorg. Chem.*, 1997, **36**, 4676.
2. C. Z. Wang, J. H. Lan, Y. L. Zhao, Z. F. Chai, Y. Z. Wei and W. Q. Shi, *Inorg Chem*, 2013, **52**, 196.